

Hard and soft methods for prediction of antioxidants' activity based on the DSC measurements

Alexey L. Pomerantsev*, Oxana Ye. Rodionova

Institute of Chemical Physics RAS, 4 Kosygin St., Moscow, 119991, Russia

Received 17 March 2005; received in revised form 11 April 2005; accepted 11 April 2005

Available online 31 May 2005

Abstract

Testing of antioxidants' activity in polyolefin is considered. It is proposed to substitute the conventional Long Term Heating Aging (LTHA) test for the method of Differential Scanning Calorimetry (DSC). Values of the Oxidation Initial Temperature measured by the DSC method (X data) are calibrated using the values of Oxidation Induction Period obtained in the LTHA tests (data Y). This data is further processed applying both soft and hard modeling. The hard method is the Non-Linear Regression approach with the traditional confidence interval estimation. The soft method combines the Partial Least Squares regression and the method of Simple Interval Calculation. We compare the results of soft and hard prediction based on the same data set and point out which approach is better in various cases.

© 2005 Elsevier B.V. All rights reserved.

Keywords: Antioxidant activity; Differential Scanning Calorimetry; Long Term Heating Aging; Interval estimations; SIC; PLS; Fitter

1. Introduction

Testing the activity of *antioxidants* (AO) in polyolefin is a long and costly process, which requires 1–3 months of heating up the samples in an oven. This laborious procedure is called Long Term Heating Aging (LTHA). This paper considers an alternative chemometric approach that makes the process of the AO development more effective. The proposal to use the Differential Scanning Calorimetry (DSC) method and to construct a calibration model that can predict AO activity has been studied earlier [1,2]. These

works describe the hard (NLR) [1] and the soft (PLS) [2] approaches to modeling, but use short data sets, different for each case. In this paper we study a representative AO sample set that enables us to explore two important issues. The first one is a practical question regarding feasibility of the suggested DSC alternative method. The second one is the comparison of the hard and the soft modeling being applied to the same data set.

The hard method is based on the Non-Linear Regression (NLR) approach [4], while the soft method employs the Projection on Latent Structures (PLS) technique [5]. Both methods give point estimates for a predicted value. To make the prediction more comprehensive for each predicted value we provide an interval that represents the uncertainty in prediction. For the hard method it is a traditional confidence interval calculated by statistical simulation. For the soft method a novel approach called Simple Interval Calculation (SIC) [6,7] is used. There are many alternative methods for calculation of uncertainty in PLS [8,9] and the literature references listed herein. Though these methods are still under discussion, we neither criticize them, nor compare them with the SIC approach. That might be an interesting

Abbreviations: AO(s), Antioxidant(s); CI(s), Confidence interval(s); DSC, Differential Scanning Calorimetry; LTHA, Long Term Heating Aging; MED, Maximum Error Deviation; NLR, Non-Linear Regression; OIP, Oxidation Induction Period; OIT, Oxidation Initial Temperature; OSP, Object Status Plot; PI(s), Prediction interval(s); PLS, Partial Least Squares; PP, Polypropylene; RMSEC, Root Mean Square Error of Calibration; RMSEP, Root Mean Square Error of Prediction; SIC, Simple Interval Calculation.

* Corresponding author. Fax: +7 95 9397483.

E-mail address: forecast@chph.ras.ru (A.L. Pomerantsev).

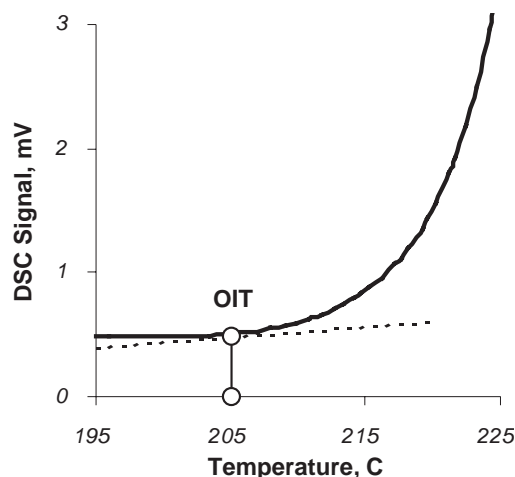


Fig. 1. Example of the DSC curve and the OIT value.

topic for the future papers, but in the present work we concentrate on comparison of the SIC method with the well-known technique of the confidence estimators in the Non-Linear Regression [10].

Antioxidant is a special additive which inhibits polymers thermo-aging, protecting polymers from oxidation during processing as well as at the end-use application. Reacting with free radicals, AO terminates chains and exhausts. The oxidation is completely suppressed as long as the concentration of AO exceeds some critical value. Therefore, it is very important to estimate Oxidation Induction Period (OIP)—the time during which the concentration of AO is high enough. The more effective is an antioxidant the longer is the OIP. In practice, the AO effectiveness is measured by the OIP value in days. A generally adopted testing procedure involves keeping polymer samples in ovens at a standard temperature like 140 °C for some time: from 1–2 days for poor AOs, up to 40 days for the AO of the best composition. Twice a day a qualified tester examines the samples and checks for apparent signs of degradation: brittleness, crumbling, yellowing. Needless to say this type of testing is very erratic and time-consuming.

An alternative to the LTHA testing is the DSC measurement and further data processing. Differential Scanning Calorimetry is a method of testing in which a sample is heated at a constant heating rate using special instruments. The measured signal represents a heat flow as a function of growing temperature T , Fig. 1. For a chemical reaction with a thermal effect, the DSC signal is proportional to the rate of the reaction. While the AO concentration in a sample is sufficient, the signal remains constant; at some specific temperature it starts growing. This temperature is called Oxidation Initial Temperature (OIT) and it is used in our example here. The DSC approach has an apparent advantage of being a fast and well-automated method without strong requirements to the size and form of specimens.

2. Experimental

The experiment is conducted using 25 AO samples marked AO-1, . . . , AO-25. Some of them (e.g. AO-1, AO-2 and AO-3) are the standard additives used in production. Other AOs are the trial agents that are expected to be effective. All samples are added to polypropylene (PP) powder in concentrations of 0.05% (500 ppm), 0.07%, and 0.1%. After blending the additive and the polymer, the mixture is added to the pre-heated extruder at the temperature of 250 °C. The product of extrusion is converted into the 0.25 mm film, which serves as a base material for the LTHA and the DSC testing.

The LTHA tests are performed at the temperature of 140 °C and result in a set of the corresponding OIP values (in days). The DSC measurements are conducted at the temperature range of 150 °C to 300 °C, where an exothermic maximum related with polymer oxidization is observed. We use five different heating rates: 2, 5, 10, 15, 20 (degree per min). The OIT values are calculated applying Fitter software [3] to the raw DSC curves as it is explained in Ref. [4].

The obtained data are shown sketchy in Fig. 2. X are the OIT values resulting from the DSC experiment. They form a 3D block: 25 AO samples \times 3 AO concentrations \times 5 heating rates. Y are the OIP values obtained in the LTHA tests. They form a 2D matrix: 25 AO samples \times 3 AO concentrations.

3. Soft modeling

This dataset is processed using a soft approach that combines the PLS method [5] for calibration and the SIC method [6] for an interval prediction, which is explained below.

The raw X data are unfolded over five heating rates as it is shown in Fig. 3. This simple method of a 3-way data modeling was applied for the reason that more complicated approaches (i.e. PARAFAC [11]) did not provide us with an

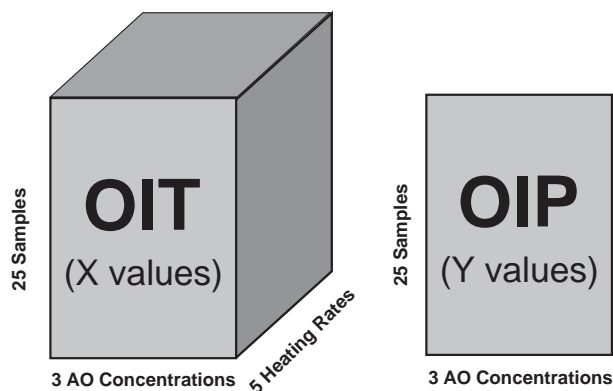


Fig. 2. Scheme of data.

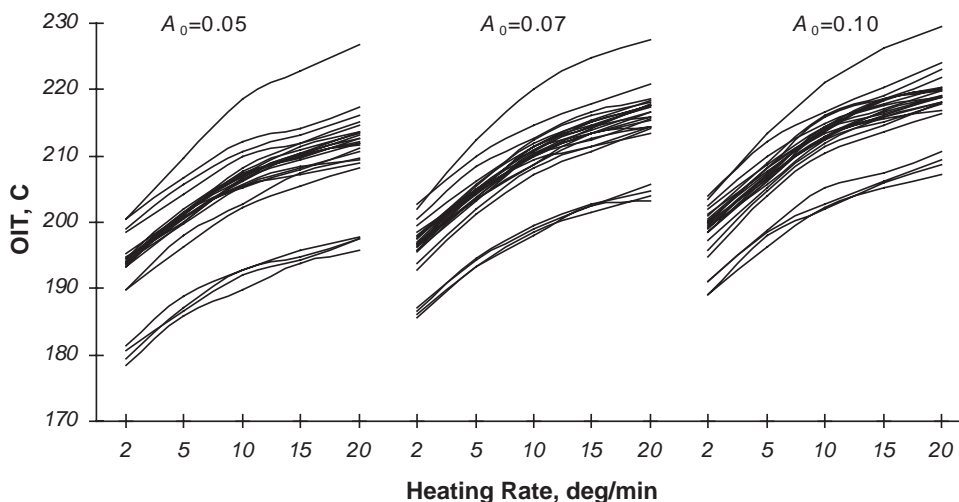


Fig. 3. X data layout for the PLS modeling.

essential gain. It is important that the variance of the OIP value is not a constant; it grows with OIP. This could be explained by two reasons. The first one is the above-mentioned method of visual inspection that provides a lower accuracy for more stable (and thus, the long-lived) AOs. The second reason is the sample preparation procedure, which implies that a small quantity of AO powder is mixed with a large amount of PP powder. It causes a certain unavoidable mixing inhomogeneity of AO in PP. To compensate for this heteroscedasticity we perform the square root transformation of the OIP values. Both X and Y are centered at the PLS modeling.

The whole data set is divided into two sample subsets. A *calibration set* consists of 18 samples (AO-1–AO-18); this set is used for modeling. The second set, which is the *test set* (AO-19–AO-25), consists of seven samples and is used for validation. For each initial AO concentration value A_0 , a separate PLS1 model with two principal components is employed. Some general characteristics of the PLS models are presented in Table 1. This table shows the explained X and Y variances, the Root Mean Square Error of Calibration, the correlation coefficients for the calibration and the test sets (for prediction vs. measurement dependence). The last column represents the SIC error of calibration that is explained below.

Using PLS, we obtain a point estimate of the OIP value. An interval estimate is obtained using the SIC method. The SIC approach is based on a single assumption that all errors ε involved in a linear calibration problem $y = \mathbf{x}^t \mathbf{a} + \varepsilon$, are

limited (sampling errors, measurement errors, modeling errors, etc.), which appears to be a reasonable supposition in many practical applications. This assumption means that there exists a positive β value (initially unknown), such that

$$\text{Prob}\{|\varepsilon| > \beta\} = 0, \quad \text{and for any } 0 < b < \beta \quad \text{Prob}\{|\varepsilon| > b\} > 0 \quad (1)$$

where $\text{Prob}\{\bullet\}$ denotes the probability that an event occurs. This value, β , is called Maximum Error Deviation (MED) and it characterizes the calibration error. An estimate of β can be found using the conventional statistic methods [6], which are applied to the regression residuals. The MED values calculated for our data are presented in the last column of Table 1.

Relying on assumption in Eq. (1), and employing a given calibration data set \mathbf{X} , \mathbf{y} with n samples, it is possible to build the entire system of inequalities regarding the unknown regression parameters \mathbf{a} ,

$$A = \{\mathbf{a} \in \mathbf{R}^p : \mathbf{y}^- < \mathbf{X}\mathbf{a} < \mathbf{y}^+\}.$$

Here $y_j^- = y_j - \beta$, $y_j^+ = y_j + \beta$, $j = 1, \dots, n$. A is a closed convex set in the parameters' space; it is called the *Region of Possible (parameter) Values (RPV)*. This is a volumetric analogue of the conventional parameter point estimates vector $\hat{\mathbf{a}}$, which is calculated with the help of any traditional regression method, e.g. PLS.

Using the obtained RPV it is possible to solve the prediction problem for any given predictor vector \mathbf{x} (e.g. a new spectrum or similar). It is clear that when parameter \mathbf{a} varies over RPV A , the corresponding predicted value $\hat{y} = \mathbf{x}^t \mathbf{a}$ belongs to an interval

$$V = [v^-, v^+] \quad (2)$$

where

$$v^- = \min_{\mathbf{a} \in A} (\mathbf{x}^t \mathbf{a}), \quad v^+ = \max_{\mathbf{a} \in A} (\mathbf{x}^t \mathbf{a}).$$

Table 1
General characteristics of the PLS models for the different initial AO concentrations

| A_0 | X_{expl} (%) | Y_{expl} (%) | RMSEC | r^2 (cal) | r^2 (test) | β |
|-------|-----------------------|-----------------------|-------|-------------|--------------|---------|
| 0.05 | 99 | 92 | 0.287 | 0.96 | 0.99 | 0.84 |
| 0.07 | 99 | 88 | 0.342 | 0.93 | 0.99 | 1.02 |
| 0.10 | 99 | 84 | 0.395 | 0.91 | 0.97 | 1.20 |

These equations represent a standard linear programming problem [12]. It is known that an extreme of bilinear form $x^t a$ is achieved at one of the vertices of convex set A . A standard numerical analysis technique (Simplex algorithm) helps us to move from one vertex to another in the direction of maximum change (increase or decrease) of the form, and enables to perform the optimization in such a way that there is no need to construct RPV explicitly. However, the limited solutions of a linear programming problem can be found if and only if (iff) the set A is bounded. It is known that A is bounded iff X is a full-rank matrix [12]. In the opposite case it is necessary to apply a regularization procedure, e.g. the PLS projection, and use a score matrix T instead of X in the SIC method further on. The SIC prediction interval (PI) V stands in contrast to the more traditional CI (confidence interval) estimators that are based on the theoretical error distributional model assumptions. The plausibility of using the latter for practical data analysis of real-world technological and natural systems is often put into doubt. Theoretical study of the CI/PI relations has been started in Ref [6,7]. The present paper draws attention to a case study that demonstrates the reasonable interrelations between CIs and PIs for a real world example.

Fig. 4 presents the results of the PLS/SIC prediction applied to the data in question. There predicted OIP values are plotted against the corresponding measured reference values in the square root transformed coordinates. Each sample (open dots are the calibration samples and black dots

are the test samples) is shown together with two error bars. Horizontal bars represent the error intervals for the measured values; these intervals are equal to the doubled MED value, β , for all samples. Vertical bars correspond to PIs (Eq. (2)); they are different for different samples. It is worth to mention that every PI is less than, or equal to the MED interval for each calibration sample. This follows from the general SIC theory (see Eq. (1)).

4. Hard modeling

The hard models for the OIP prediction are constructed for each AO individually. The calibration procedure consists of two steps. At the first step a model that describes AO consumption in the course of the DSC testing is built. It is an implicit function of OIT value T , initial AO concentration A_0 , and heating rate v . This function nonlinearly depends on the unknown parameters that are estimated using NLR. At the second step a model for the AO consumption during the LTHA tests is built. The model predicts the OIP value as an explicit function of the exposition temperature T and the initial AO concentration A_0 . This function depends on the same parameters that have been estimated at the first step, so a special error propagation procedure is applied to obtain the uncertainty of the predicted OIP.

Let us consider the first step of modeling. In the course of material aging AO is exhausted. OIP is defined as a moment of time when the AO concentration reaches some critical

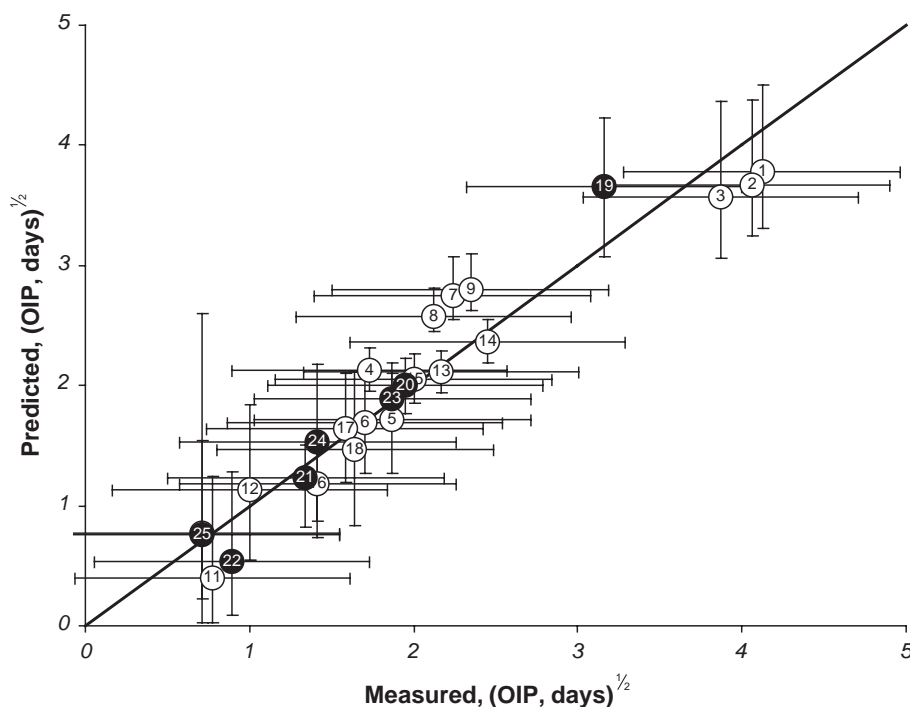


Fig. 4. Prediction of the OIP values by the soft method. Predicted values vs. measured values in the square root transformation for the data set with initial AO concentration of 0.05. Open dots (○) represent calibration samples and black dots (●) are test samples. Horizontal bars show β (calibration) error, vertical bars show the SIC (prediction) intervals.

value A_c , which depends on temperature by the Arrhenius law [13]

$$A_c = k_c \exp\left(-\frac{E_c}{RT}\right) \quad (3)$$

The heating consumption of AO can be expressed by a kinetic equation

$$\frac{dA}{dt} = -kA$$

$$A(0) = A_0 \quad (4)$$

where $A=A(t)$ is the current AO concentration, A_0 is the initial AO concentration, k is the rate constant that also depends on temperature by the Arrhenius law

$$k = k_a \exp\left(\frac{-E_a}{RT}\right).$$

In the DSC experiment, the specimens are heated at a constant heating rate v starting from the room temperature $T_0=293$ K, i.e.

$$T(t) = T_0 + vt.$$

In such a case, the solution of Eq. (4) may be presented as

$$A(t) = A_0 \exp(-k_0 Z(t)) \quad (5)$$

where function

$$Z(t) = \int_0^t \exp\left(-\frac{E_a}{R(T_0 + vs)}\right) ds$$

may be expressed using the standard [14] integral exponential function $E_n(z)$, which is defined as

$$E_n(z) = \int_1^\infty t^{-n} e^{-zt} dt, \quad n = 0, 1, 2, \dots; \quad z > 0.$$

It is convenient to represent Z as a function of temperature T rather than time t

$$Z(T) = \frac{1}{v} \left[TE_2\left(\frac{E_a}{RT}\right) - T_0 E_2\left(\frac{E_a}{RT_0}\right) \right]. \quad (6)$$

Substituting Eq. (6) into Eq. (5) and equating AO concentration $A(t)$ to the critical concentration A_c (see Eq. (3)) one obtains an equation

$$A_0 \exp(-k_0 Z(T)) = k_c \exp\left(-\frac{E_c}{RT}\right) \quad (7)$$

that implicitly determines the value of OIT, T . A more convenient form that is used for the parameter estimation follows from taking the logarithm of Eq. (7) and after some simplifications

$$\exp(a) E_2\left(\frac{E_a}{RT}\right) T + v \left(c - a - \frac{E_c}{RT} \right) = 0, \quad (8)$$

where $a = \ln(k_a)$, and $c = \ln(k_c)$.

In this equation, T is a response (OIT); a , E_a , c , and E_c are the unknown parameters; v (heating rate) and A_0 (initial concentration) are predictors. In data processing Eq. (8) should be solved with respect to the response variable T

$$T = T(v, A_0; a, E_a, c, E_c) \quad (9)$$

repeatedly, at any given values of predictors v and A_0 . This solution is used in the search for such values (the estimates) of parameters a , E_a , c , and E_c that minimize the sum of least squares

$$\min_{a, E_a, c, E_c} \sum_{ij} [Y_{ij} - T(v_j, A_{0i}; a, E_a, c, E_c)]^2. \quad (10)$$

Here Y_{ij} are the experimental OIT values, index i stands for the three initial AO concentrations A_0 , and index j numerates five heating rates v .

The minimization of the sum (10) is connected with the following problems. First of all, the regression function (9) cannot be presented explicitly, or even expressed implicitly using elementary functions. Secondly, Eq. (8) undoubtedly represents a function that is non-linear with respect to its unknown parameters. At last, minimization of sum (10) is a *stiff* problem. The stiffness of fitting problem

$$\min_{\theta} S(\theta), \quad \text{where } S(\theta) = (\mathbf{y} - \mathbf{f}(\theta))^2,$$

(also called as *multicollinearity*) can be characterized via a span of eigenvalues λ of the Hesse matrix \mathbf{H}

$$\text{NA}(\mathbf{H}) = \log_{10} \frac{\lambda_{\max}(\mathbf{H})}{\lambda_{\min}(\mathbf{H})}, \quad \text{where}$$

$$H_{ij} = \frac{\partial^2 S(\theta)}{\partial \theta_i \partial \theta_j} \approx 2 \left[\frac{\partial f(\theta)}{\partial \theta_i} \right]^t \frac{\partial f(\theta)}{\partial \theta_j}.$$

Here vector θ denotes the set of parameters (a , E_a , c , E_c). Matrix \mathbf{H} is inverted repeatedly in the course of fitting. To make an accurate inversion it is necessary to perform computations with NA+2 true digits at least. If the model is an implicit function $f(\theta)$, two more true digits are required; that results in NA+4 required true digits. Finally, if such a method is applied, the numerical calculation of derivatives $\partial f(\theta)/\partial \theta_i$ demands two true digits more, to a total of NA+6. In our case stiffness NA equals 7 in the point of minimum and it is about 15 in a distant starting point. Therefore, it is necessary to retain some 13–20 true digits in calculations.

All these issues turn fitting into a rather complicated problem. In order to solve it we apply a special tool, Fitter software [3], because it has the features that allow solving such kind of problems. Fitter employs a stable gradient method for minimization that is based on the matrix exponential technique [15]. The latter appears to be better than the popular Levenberg–Marquardt algorithm [16]. Secondly, in Fitter it is possible to set a regression equation in its ordinary algebraic form, which permits even implicit expressions. For example, Eq. (8) is introduced in Fitter as it is shown in Fig. 5. Here a standard built-in Fitter function

```
'OIT model
0=exp(a)*ea*ixp[ea/(T+273)]+v*[b-ec/(T+273)];200<T<300
b=c-log(A0)
ec=Ec/R
ea=Ea/R
R= 8.315E-3
a=?
Ea=?
c=?
Ec=?
```

Fig. 5. OIT model given by Eq. (8) in the form that is used in Fitter.

$\text{ixp}(x)=x^{-1}E_2(x)$ is used. From Fig. 5 one can see that the Fitter representation of the model looks rather similar to a standard mathematical notation given by Eq. (8). The third important Fitter's feature is that calculations of derivatives are carried out automatically through a symbolic computing that maintains a high precision of calculations. One example of fitting is presented in Fig. 6, which plots the experimental OIT values (dots) for AO-1 and the corresponding fitting curves.

Now we consider the second step of modeling at which we construct model that describes the AO consumption during the LTHA test. The model is used for the OIP prediction later on. This model depends on the same parameter set θ that has been estimated at the first step.

Solution of Eq. (4) at the constant conditions ($T=\text{Const}$, therefore, $k=\text{Const}$, too) is

$$A(t) = A_0 \exp(-kt).$$

To determine OIP value t_i one has to equate current AO concentration $A(t)$ to a critical value A_c defined in Eq. (3). Thus we obtain a formula for the OIP calculation

$$t_i = \left[\frac{E_c}{RT_c} + \ln(A_0) - c \right] \exp\left(\frac{E_a}{RT_c} - a \right), \quad (11)$$

where T_c is an exposition (aging) temperature. In our case it is 140 °C, so $T_c=413$ K.

In this equation, we use the parameter estimates $\hat{\theta} = (\hat{a}, \hat{E}_a, \hat{c}, \hat{E}_c)$ found at the first step of calibration. In order

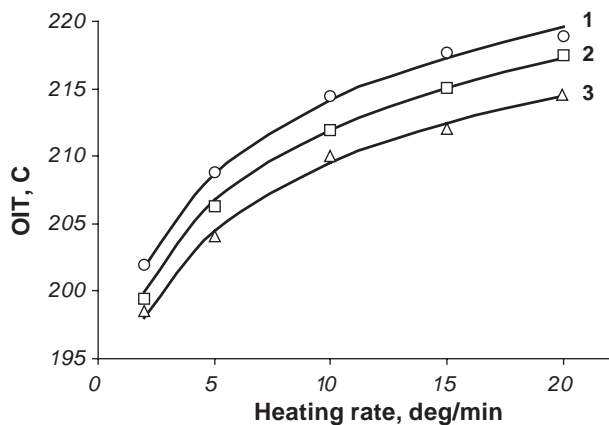


Fig. 6. OIT values (dots and curves) vs. heating rate for the different initial AO concentrations: 0.1 (1, ○), 0.07 (2, □), 0.05 (3, △). PP+AO-1.

to obtain not only the predicted OIP value, but also its confidence limits, it is necessary to take into account the uncertainties of these estimates. Unfortunately, the conventional method of error propagation

$$\text{var}(f) = \frac{\partial f(\hat{\theta})^t}{\partial \theta} \text{cov}(\hat{\theta}, \hat{\theta}) \frac{\partial f(\hat{\theta})}{\partial \theta},$$

cannot be applied to Eq. (11) due to non-linearity of the model.

The true confidence interval (CI) can be found using a statistical simulation, namely the method of free simulation [10]. In this method, the CI for the function $f(\hat{\theta})$ is calculated as a percentile of a sampling $\{f(\theta_1), f(\theta_2), \dots\}$. Sampling values $f(\theta_i)$ are obtained by simulation of parameters θ_i in accordance with normal distribution $N(\hat{\theta}, \text{cov}(\hat{\theta}, \hat{\theta}))$. An example of the confidence prediction constructed by such a technique for sample AO-18 is shown in Fig. 7. The confidence probability is $P=0.90$. The CIs for other AO samples are presented in Fig. 8.

It is important that no OIP reference values were involved in the hard (NLR) modeling. Therefore they can be used in validation, e.g. for calculation of the Root Mean Square Error of Prediction (RMSEP), which are shown in

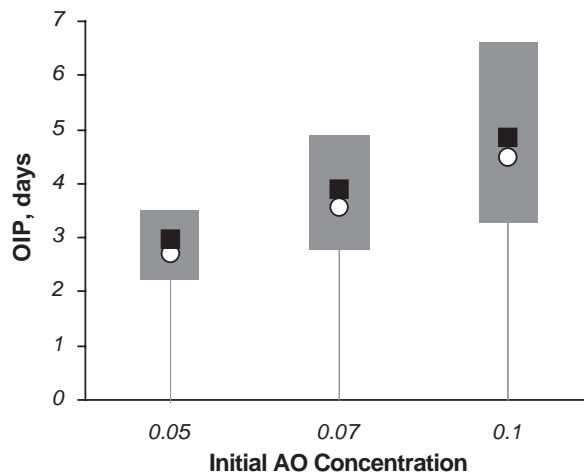


Fig. 7. Prediction of OIP for the different initial AO concentrations by the NLR method. Confidence intervals at probability $P=0.90$ are shown by the grey boxes. Black squares (■) represent the point OIP estimates and open dots (○) are the reference values. PP+AO-18.

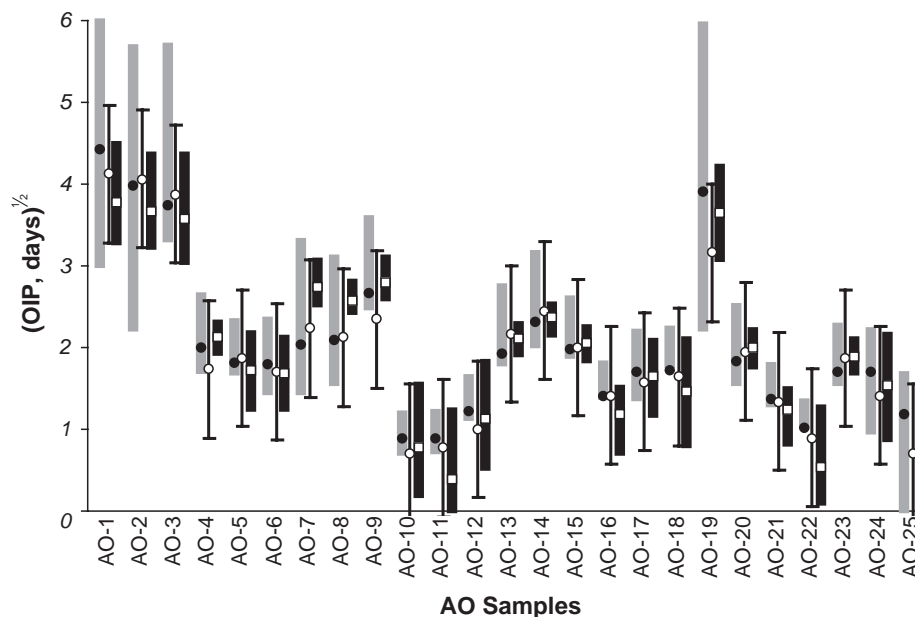


Fig. 8. The results of the OIP prediction for samples with initial AO concentration of 0.05. Black dots (●) and grey bars represent the NLR predictions. Open squares (□) and black bars stand for the PLS/SIC predictions. Open dots (○) correspond to the reference values with vertical bars that show β (calibration, or measurement) error. All values are square root transformed.

Table 2. At the same time, it is impossible to evaluate such a traditional calibration error as RMSEC (the Root-Mean Square Error of Calibration), inasmuch as at the first stage of the NLR modeling not the OIP, but the OIT values were calibrated as a function of ν and A_0 . However, it is possible to evaluate the residual sum of squares for each AO and calculate the average variance in the OIT estimates afterwards. The latter are shown in Table 2 in row 4.

5. Results and discussion

In the present section we compare the hard (NLR) models and the soft (PLS) models, which have been constructed based on the same data set. These models employ data differently. There are 25 hard models constructed for each AO, and 3 soft models build for each initial AO concentration value. In Fig. 8 the results obtained by each method for samples with initial AO concentration of

0.05 are combined. This plot shows the results of the NLR (hard) prediction (black dots and grey CI bars for confidence probability 0.90); the results of the PLS/SIC (soft) prediction (open squares and black PI bars); and the reference values (open dots) with error bars that show the MED value β (calibration error). To make the comparison of the methods clearer all values are plotted in the square root transformed OIP coordinate. Analogous plots can be constructed for other data subsets with initial concentrations of 0.07 and 0.10; they look rather similar to Fig. 8.

Table 2 presents some general statistical characteristics of the NLR and the PLS/SIC prediction results. Here the following notations for measured and predicted the X (OIT) and the Y (OIP) values are used. \mathbf{X} and $\hat{\mathbf{X}}$ are the measured and the predicted OIT values, respectively; $\mathbf{y} = \sqrt{\text{OIP}}$ is the square root transformed vector of the measured (reference) OIP values; $\hat{\mathbf{y}}_i$ are the corresponding vectors of the square root transformed point estimates of OIP obtained by the NLR ($i=1$) and by the PLS/SIC ($i=2$) methods; \mathbf{w}_i are the vectors of the widths of CIs (NLR, $i=1$) and the widths of PIs (PLS/SIC, $i=2$); all intervals are also square root transformed.

Exploring Table 2 and Fig. 8 the following conclusions can be drawn out. Both methods give a similar accuracy (see row 1 in Table 2) and bias (row 2). The quality of prediction becomes worse when initial AO concentration increases. In general, the PLS/SIC prediction gives better results for the small initial AO concentration, while NLR is better for the large concentrations. However, the point estimates are close on average (row 3). Both the NLR and the PLS methods explain the X data (i.e. the OIT values) rather similar, but NLR is slightly better (row 4).

Table 2
Statistical characteristics of prediction by the NLR and the PLS/SIC methods

| Initial AO concentration | NLR ($i=1$, CIs) | | | PLS/SIC ($i=2$, PIs) | | |
|---|--------------------|-------|-------|------------------------|--------|--------|
| | 0.05 | 0.07 | 0.10 | 0.05 | 0.07 | 0.10 |
| 1. RMSEP | 0.242 | 0.246 | 0.272 | 0.239 | 0.251 | 0.336 |
| 2. Bias | 0.087 | 0.058 | 0.040 | 0.011 | 0.004 | 0.002 |
| 3. Cor ($\hat{\mathbf{y}}_1, \hat{\mathbf{y}}_2$) | 0.953 | 0.934 | 0.916 | 0.953 | 0.934 | 0.916 |
| 4. Average $(\mathbf{X} - \hat{\mathbf{X}})^2$ | | 0.224 | | 0.286 | 0.286 | 0.286 |
| 5. Average (\mathbf{w}_i) | 1.038 | 1.151 | 1.397 | 0.934 | 1.204 | 1.476 |
| 6. Cor ($\mathbf{w}_1, \mathbf{w}_2$) | 0.202 | 0.007 | 0.028 | 0.202 | 0.007 | 0.028 |
| 7. Cor (\mathbf{y}, \mathbf{w}_i) | 0.815 | 0.846 | 0.836 | -0.184 | -0.161 | -0.113 |

The interval estimates are also very similar on average (row 5), but the NLR intervals (CIs) and the SIC intervals (PIs) are quite different for the individual samples (row 6). The last row of Table 2 shows that the width of the CIs increases with predicted value for all initial AO concentrations, while the width of the PIs does not depend on y . This testifies that the employed response transformation $y = \sqrt{\text{OIP}}$ yielded the expected result in the PLS/SIC modeling, but could not straighten the NLR prediction.

The fact that the width of all intervals grows with initial AO concentration A_0 is clearly seen from the hard model formula (Eq. (11)), which represents OIP value t in dependence of A_0 . On the other hand, in the soft PLS model one could not foresee this by any means. Nevertheless, this is obviously a fundamental feature of the explored polymeric system; i.e. the more AO is added to a sample initially, the more its OIP, and the worse is the prediction. This demonstrates that with respect to this general aspect both the soft and the hard approaches are similar in our example.

Simultaneously, one can observe that the soft and the hard prediction results differ for the individual samples. From Fig. 8 it can be seen that for some samples (e.g. AO-5, 6, 10, 11, ...) the CIs are less than the PIs, while for the other samples (e.g. AO-1, 2, 3, ...) the opposite is true. It is interesting to consider why the individual NLR and SIC intervals are so different. Fig. 9 demonstrates the PLS score plot for the samples with initial AO concentration of 0.05. Eighteen calibration samples (AO-1, ..., AO-18) are presented by the open dots and six training samples (AO-19, ..., AO-25) are marked by the closed dots. It can be seen that the test sample AO-25 is an evident outlier (or an absolute outsider in the SIC object status classification [7] terminology). The predicted value for AO-25 is rather close

to the measured value, but this sample is located very far from the center of the model. Therefore the uncertainty in prediction of AO-25 is high. This sample has the largest SIC-interval (see Fig. 8) and it is the only test sample for which the prediction error is worse than the calibration MED error.

From this plot it also can be seen that all samples, for which the NLR confidence intervals (CIs) are less than the SIC prediction intervals (PIs), are located in the bottom part of the plot, below the bold line. This line splits the samples in two groups: $\text{CIs} > \text{PIs}$ and $\text{CIs} < \text{PIs}$. This is a rather surprising outcome. This could be expected discovering of some score patterns, which are connected with the width of prediction (confidence) intervals, while actually there has been found a structure that distinguishes samples for which the hard approach is better than the soft one, and vice versa. In this case it is useful to explore another plot that represents the NLR method, and to look whether the similar patterns could be detected there.

Fig. 10 presents a plot that demonstrates correlation between the NLR estimates of parameters E_c and c (see Eq. (8)). It is worthy of mentioning that the parameter estimates in both pairs: (a, E_a) and (c, E_c) in Eq. (8) are highly correlated. It is usually the case in the Arrhenius model that correlation between the estimates of the pre-exponential factor and the corresponding activation energy is close to 1 [17]. In our case: $\text{cor}(\hat{a}, \hat{E}_a) = 0.995$, $\text{cor}(\hat{c}, \hat{E}_c) = 0.997$. Fig. 10 gives another view on the problem in question. From this plot it can be clearly seen that all samples for which the NLR approach is better ($\text{CIs} < \text{PIs}$) are situated at the bottom part of the plot, below the bold line, and vice versa. The transition corresponds to critical AO concentration A_c (Eq. (3)) that is equal to 0.013 at $T = 140$ °C.

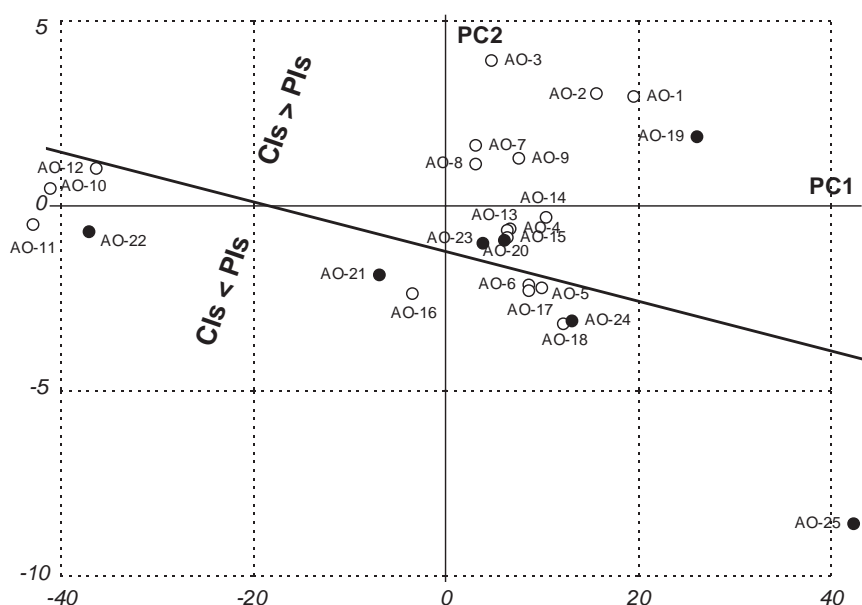


Fig. 9. PLS score plot for samples with initial AO concentration of 0.05. Open dots (○) represent calibration sample and black dots (●) represent test samples. Bold line separates the samples for which the NLR confidence intervals (CIs) are less (greater) than the SIC prediction intervals (PIs).

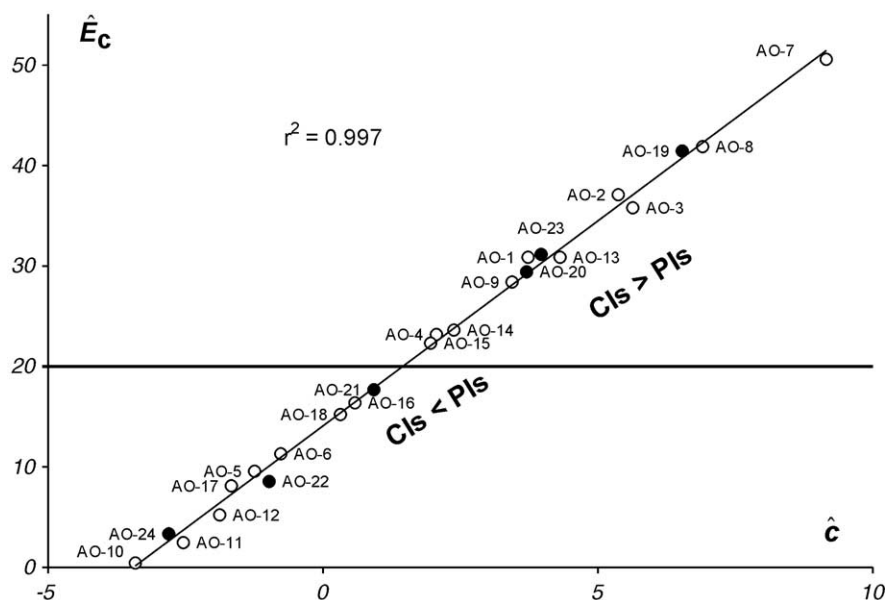


Fig. 10. Correlation between the estimates of pre-exponential c and corresponding activation energy E_c in Eq. (3). Open dots (○) represent calibration samples and black dots (●) represent test samples. Thin line shows the linear correlation trend. Bold line separates samples for which the NLR confidence intervals (CIs) are less than the SIC prediction intervals (PIs).

Score plot in Fig. 9 is constructed only for a single sample subset, namely for the samples with initial AO concentration $A_0=0.05$. The score plots for the subsets with $A_0=0.07$, and $A_0=0.10$ have a structure that is similar to one in Fig. 9. On the other hand, the estimates of parameters (c , E_c) were obtained in the hard modeling wherein all samples with all initial AO concentrations are processed together in each NLR model; so the plot in Fig. 10 represents the whole data set. This reason enables us to claim the following conclusion, which is important for the choice of the calibration method. Such property as: “the NLR confidence interval (CI) is less/greater than the SIC prediction interval (PI)” does not depend on the initial AO concentration in a sample, but subjects to the critical AO concentration, which is an internal characteristic of AO itself.

Another important issue that could be considered in the context of the methods comparison is the restriction of the areas where these methods are valid and applicable. The hard (NLR) approach has an evident advantage being applicable to prediction of OIP at the various temperature and concentration conditions. Fig. 11 presents a plot in which OIP is predicted for the temperature range $80^\circ\text{C} < T < 200^\circ\text{C}$ at initial AO concentration $A_0=0.04$. Needless to say that these conditions were not explored during the experiments and the results are calculated just by extrapolation of Eq. (9) to the setting. Certainly with the soft (PLS) modeling such an outcome cannot be obtained by any means. Incidentally, temperature $T=200^\circ\text{C}$ is of great importance as it is the PP processing temperature at which the polymer is extruded. On the other hand it is rather risky to apply the NLR model for a condition that is too far from the experimental values. In particular the model cannot be

extrapolated to the room temperature, and therefore it is impossible to forecast a long-term PP storage using the DSC measurements. These cautious words actually mean that it is impossible to fix the strict limits in which the NLR approach is valid.

For the PLS/SIC approach the situation is quite different. Here we can claim the proper limits of applicability. Fig. 12 demonstrates the SIC Object Status Plot (OSP) that is used for such a restraint. The complete explanation of the OSP technique is given in Ref. [7], so here we present only a short description. Each test sample is plotted with its OSP coordinates that are as follows. The SIC-residual is the difference between the center of the PI

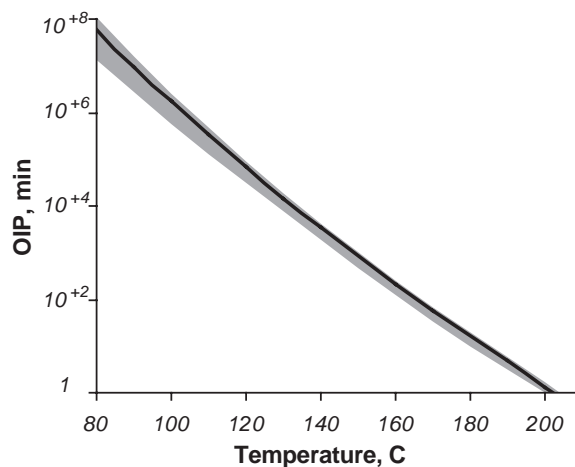


Fig. 11. Prediction of the OIP values at the different exposition temperatures for AO-18 with initial concentration 0.04. Bold line represents the mean value and the grey-shaded corridor shows the 0.95 confidence intervals.

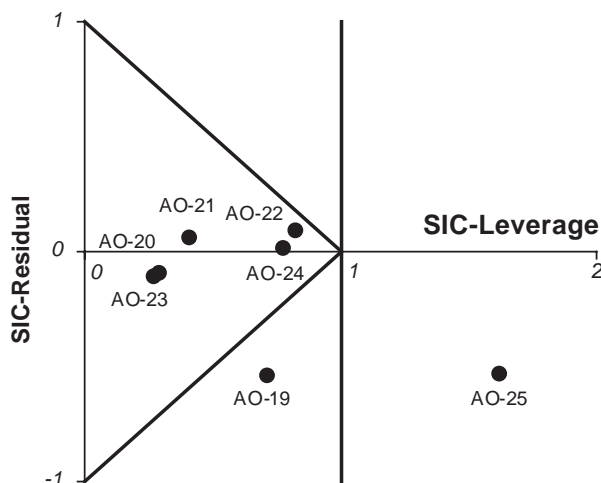


Fig. 12. SIC Object Status Plot (OSP) for the test samples with $A_0=0.07$.

and the reference value, scaled with β . The *SIC-leverage* is the width of PI, also divided by β . The position of a test (or a new) sample in OSP determines its applicability in prediction. All samples that are located inside the triangle (AO-21, ..., AO-24) are called *insiders*. They agree with the model completely; thus insiders can be mostly trusted in prediction. The opposite case means that objects are located *outside* the existing model, therefore they are termed *outsiders* (samples AO-19 and AO-25). The outsiders do not contradict the model but they are less-than-perfect with respect to prediction. There may be two reasons for this: either the width of PI is greater than the calibration error (sample AO-25), or there is a bias (sample AO-19). Hence using the OSP technique one can easily classify a new sample and in that way strictly limits the area in which the PLS/SIC approach is valid.

Discussing the conditions under which a method of modeling is valid it is necessary to mention the different nature of the areas of applicability. In the hard approach this is the area of predictors (T and A_0) wherein the model might be extrapolated when applied to the same AO sample as explored in the DSC experiment. In the soft approach this is the area of new AOs for which the constructed soft model is valid. Obviously, the predictor values, i.e. the initial AO concentrations and the DSC heating rates should be equal to those in the training set.

One more important issue is worth mentioning. Different designs of experiments should be applied when a more accurate model is to be acquired. In the case of the soft modeling it is possible to improve the model and the prediction accuracy by adding more samples to the calibration set. In the case of the hard modeling it is necessary to construct a special model for each AO, meaning that the model can be improved by conducting more experiments with various concentrations for a given AO. Apparently this improves the model accuracy for a given AO and has no influence on the prediction accuracy for other AOs.

6. Conclusions

The research described in the present paper led to the following conclusions.

- 1) It has been shown that a long and costly LTHA process of the AO activity testing can be replaced with a fast DSC technique with further data processing by the hard (NLR) or by the soft (SIC/PLS) methods. Both calibration approaches give a satisfactory accuracy of the OIP prediction that is not worse than the LTHA measurement error. Therefore we could recommend these methods for practical implementation.
- 2) Each calibration method has its own advantages and disadvantages. The hard approach enables us to obtain the prediction results extrapolated to the conditions (temperature and concentration) beyond the area of the experiments. However, it is impossible to restrict the borders of such an extrapolation, and sometimes this outcome is not trustworthy enough. On the contrary, the soft method has a strict area of application that is outlined with the help of the OSP technique. At the same time the PLS/SIC approach cannot be applied to predict OIP at the conditions that differ from the conditions used in the calibration experiments.
- 3) Both calibration methods have a similar quality of prediction and reveal a parallel behavior with respect to the conditions of prediction, e.g. the greater the initial AO concentration, the worse the accuracy of prediction. However, the hard approach is better for AOs with a lower value of the critical AO concentration, i.e. for AOs with the small OIP values, while the soft method is better in the opposite case. This is a fundamental inherent feature of AOs that remains even at the change of the initial AO concentration in a sample.
- 4) The application of the hard modeling is preferable when the aim of investigation is the prediction of a given polymer system behavior. In case a researcher wants to compare the activity of different AOs, the soft model approach meets the investigation goal better.

References

- [1] E.V. Bystritskaya, A.L. Pomerantsev, O.Ye. Rodionova, CONFERENCE CHEMOMETRICA (CC-97), Budapest, (1997). <http://sol.cc.u-szeged.hu/~rajko/Pos54.gif>.
- [2] A.L. Pomerantsev, O.Ye. Rodionova, in: Zaikov, et al. (Ed.), Aging of Polymers, Polymer Blends and Polymer Composites, vol. 1, NovaScience Publishers, New York, 2002, pp. 19–29.
- [3] Fitter Add-In., <http://polycert.chph.ras.ru/fitter.htm> [1 May 2004].
- [4] E.V. Bystritskaya, A.L. Pomerantsev, O.Ye. Rodionova, J. Chemom. 14 (2000) 667–692.
- [5] A. Höskuldsson, Prediction Methods in Science and Technology, Thor Publishing, Copenhagen, Denmark, 1996.
- [6] O.Ye. Rodionova, A.L. Pomerantsev, in: Pomerantsev (Ed.), Progress in Chemometrics Research, NovaScience Publishers, New York, 2005, pp. 43–64.

- [7] O.Ye. Rodionova, K.H. Esbensen, A.L. Pomerantsev, *J. Chemom.* 18 (2004) 402–413.
- [8] M. Høy, K. Steen, H. Martens, *Chemometr. Intell. Lab. Syst.* 44 (1998) 123–133.
- [9] J.A. Fernández Pierna, L. Jin, F. Wahl, N. Faber, D.L. Massart, *Chemometr. Intell. Lab. Syst.* 65 (2003) 281–291.
- [10] A.L. Pomerantsev, *Chemometr. Intell. Lab. Syst.* 49 (1999) 41–48.
- [11] A. Smilde, R. Bro, P. Geladi, *Multi-Way Analysis with Applications in the Chemical Sciences*, John Wiley Sons, Chichester, 2004.
- [12] H. Taha, *Operations Research. An Introduction*, 3rd ed., Macmillan Publishing Co., New York, 1982.
- [13] Yu.A. Shlyapnikov, *Development in Polymer Stabilization*, vol. 5, Applied Science Publishers, London, 1981, pp. 1–22.
- [14] M. Abramowitz, I. Stegun, *Handbook of Mathematical Functions*, National Bureau of Standards, 1964.
- [15] B.V. Pavlov, A.Ya. Povzner, *Z. Vychisl. Mat. Mat. Fiz.* 13 (1973) 1056–1059.
- [16] D.W. Marquardt, *SIAM J.* 11 (1963) 431–441.
- [17] O.Ye. Rodionova, A.L. Pomerantsev, Estimation of the Arrhenius parameters, *Kinet. Katal.*, in print.